Influenza Hemagglutinin-mediated Fusion Pores Connecting Cells to Planar Membranes: Flickering to Final Expansion

GRIGORY B. MELIKYAN,* WALTER D. NILES,* MARK E. PEEPLES,‡ and FREDRIC S. COHEN*

From the Departments of *Physiology and ‡Immunology/Microbiology, Rush Medical College, Chicago, Illinois 60612

ABSTRACT We have studied the fusion between voltage-clamped planar lipid bilayers and influenza virus infected MDCK cells, adhered to one side of the bilayer, using measurements of electrical admittance and fluorescence. The changes in currents in-phase and 90° out-of-phase with respect to the applied sinosoidal voltage were used to monitor the addition of the cell membrane capacitance to that of the lipid bilayer through a fusion pore connecting the two membranes. When ethidium bromide was included in the solution of the cell-free side of the bilayer, increases in cell fluorescence accompanied the admittance changes, independently confirming that these changes were due to formation of a fusion pore. Fusion required acidic pH on the cell-containing side and depended on temperature. For fusion to occur, the influenza hemagglutinin (HA) had to be cleaved into HA1 and HA2 subunits. The incorporation of gangliosides into the planar bilayers greatly augmented fusion. Fusion pores developed in four distinct stages after acidification: (*a*) a pre-pore, electrically quiescent stage; (*b*) a flickering stage, with 1–2 nS pores opening and closing repetitively; (*c*) an irreversibly opened stage, in which pore conductances varied between 2 and 100 nS and exhibited diverse kinetics; (*d*) a fully opened stage, initiated by an instantaneous, time-resolution limited, increase in conductance leveling at ~500 nS. The expansion of pores by stages has also been shown to occur during exocytosis in mast cells and fusion of HA-expressing cells and erythrocytes. We conclude that essential features of fusion pores are produced with proteins in just one of the two fusing membranes.

INTRODUCTION

Membrane fusion is characterized by a pore connecting the two formerly separate aqueous compartments, as the two bilayers merge. The early fusion pores have been

Dr. Melikyan's permanent address is Orbeli Institute of Physiology, 22 Orbeli Street, Yerevan, 375028, Armenia.

Address correspondence to Dr. Fredric S. Cohen, Department of Physiology, Rush Medical College, 1653 West Congress Parkway, Chicago, IL 60612.

J. GEN. PHYSIOL. © The Rockefeller University Press · 0022-1295/93/12/1131/19 $2.00
Volume 102 December 1993 1131–1149

readily detected by time-resolved admittance measurements (Zimmerberg, Curran, Cohen, and Brodwick, 1987), and the technique has been extensively used to study pores in exocytotic secretion (Breckenridge and Almers, 1987; Alvarez de Toledo and Fernandez, 1988; Spruce, Breckenridge, Lee, and Almers, 1990; Monck, Alvarez de Toledo, and Fernandez, 1990; Curran, Cohen, Chandler, Munson, and Zimmerberg, 1993) and in influenza hemagglutinin-mediated cell-cell fusion (Spruce et al., 1989, 1991). But because fusion pores are localized and transient, their structures and even their compositions are uncertain. It has been conjectured that they are composed solely of proteins (Almers and Tse, 1990), protein and lipid (Zimmerberg, Curran, and Cohen, 1991), or only lipid (Bentz, Ellens, and Alford, 1990; Stegmann, White, and Helenius, 1990; Nanavati, Markin, Oberhauser, and Fernandez, 1992). To further study the nature of fusion pores, we have fused cells to planar lipid bilayers. This system allows for high time resolution measurements and manipulation of the composition of one of the fusing membranes.

The best characterized fusion protein is influenza virus hemagglutinin (HA), a homotrimeric glycoprotein that regulates both binding and fusion of virus envelope to the target membrane (White, 1992; White, Kielian, and Helenius, 1983). The ectodomain of this integral membrane protein has a crystallographically known structure (Wilson, Skehel, and Wiley, 1981; Weis, Brown, Cusack, Paulson, Skehel, and Wiley, 1988), making it an excellent protein for structure-function studies. HA is synthesized as an inactive HA0 precursor which is proteolytically cleaved into its fusogenic form of HA1, HA2 subunits linked by a disulfide bond (Wiley and Skehel, 1987). Influenza virus enters the endocytotic pathway (Matlin, Reggio, Helenius, and Simons, 1981; Huang, Rott, and Klenk, 1981; Yoshimura, Kuroda, Kawasaki, Yamashina, Maeda, and Ohnishi, 1982) after its HAs bind to cell membrane receptors, namely sialic acid containing glycolipids and glycoproteins (Suzuki, Nagao, Kato, Matsumoto, Nerome, Nakajima, and Nobusawa, 1986). The low pH within endosomes induces a conformational change of the HA (Skehel, Bayley, Brown, Martin, Waterfield, and White, 1982; Yewdell, Gerhard, and Bachi, 1983; Doms, Helenius, and White, 1985; White and Wilson, 1987): the hydrophobic NH_2-terminus of HA2 (the fusion peptide) sequestered from water at neutral pH, becomes exposed at acidic pH and inserts into the host membrane (White and Wilson, 1987; Harter, James, Bachi, Semenza, and Brunner, 1989; Brunner, Zugliani, and Mischler, 1991; Stegmann, Delfino, Richards, and Helenius, 1991). Insertion leads to fusion between the envelope and endosomal membrane with the release of the viral genome into the cytosol and consequent cellular infection (Matlin et al., 1981; Yoshimura et al., 1982; Yoshimura and Ohnishi, 1984; Stegmann, Morselt, Scholma, and Wilschut, 1987). Low pH also induces fusion between virus and plasma membranes of cells (Huang, Dietsch, and Rott, 1985; Georgiou, Morrison, and Cherry, 1989; Lowy, Sarkar, Chen, and Blumenthal, 1990) and between virus and liposomes (Hoekstra, de Boer, Klappe, and Wilschut, 1984; Stegmann, Nir, and Wilschut, 1989). In fact, any membrane containing HA (for instance, a cell membrane expressing HA) will fuse to a target membrane when the bathing solution is at low pH (White, Helenius, and Gething, 1982; van Meer and Simons, 1983; Ellens, Bentz, Mason, Zhang, and White, 1990). Here we show that cells with HAs in their membranes fuse to planar bilayer membranes and the pores can be followed from formation to final expansion.

MATERIALS AND METHODS

Cells and Virus

Madin-Darby canine kidney (MDCK) cells were maintained in RPMI-1640 medium (Gibco Laboratories, Grand Island, NY) supplemented with 10% fetal bovine serum, 25 mM HEPES, 110 U/ml penicillin, 100 μg/ml streptomycin (van Meer and Simons, 1983). Fibroblasts transfected with HA, cell line NIH3T3-HAb2 (Doxsey, Sambrook, Helenius, and White, 1985) provided by J. White (U of California at San Francisco, CA), were cultured in DMEM medium (Gibco Laboratories) supplemented as above. When HAb2 cells with uncleaved HA0 were required, they were released from the plastic dish by incubating in a trypsin-free, phosphate buffered solution (PBS) with 0.5 mg/ml EDTA and 0.5 mg/ml EGTA for 10 min at 37°C. Influenza virus strains A/Japan/305/57 (inoculum provided by R. Webster, St. Jude Children's Research Hospital, Memphis, TN) and A/PR/8/34 were grown in the allantoic cavity of 10-d embryonated chicken eggs and harvested 56–60 h post infection. Plaque-forming units (pfu) of the harvested viral stock were determined on MDCK cells (Matlin and Simons, 1983).

Infection

Confluent monolayers of MDCK cells in 60-mm culture dishes were infected with strains A/Japan/305/57 (2–3 pfu/cell) or A/PR/8/34 (10–12 pfu/cell) for 1 h at 37°C, 5% CO_2 in serum-free DMEM medium. The virus solution was replaced by the regular medium and the cells were incubated for an additional 5 h. At that time, there were many budding and fully assembled viral particles as well as diffusely distributed envelope glycoproteins on the cell surface (Boulan and Pendergast, 1980; van Meer and Simons, 1983). The cells were lifted from the culture dish and the viral HA0 glycoproteins were activated by incubating in a 0.5 mg/ml trypsin (TPCK treated, Sigma Chemical Co., St. Louis, MO), 0.2 mg/ml EDTA solution for 5 min at 37°C. The reaction was stopped with an excess of soybean trypsin inhibitor (Sigma Chemical Co.), the cells were washed three times, and resuspended in PBS at 3– 5 × 10^7 cells/ml. This concentrated cell suspension was stored on ice and used within 6 h. Control experiments showed that activity was constant over this 6 h period. HA expression and fusogenic activity were monitored by binding and fusing infected cells to octadecylrhodamine (R18) labeled human erythrocytes (Morris, Sarkar, White, and Blumenthal, 1989).

Planar Membranes

Solvent-free horizontal planar lipid bilayer membranes were formed from a squalene solution of dioleoylphosphatidylcholine (DOPC)/bovine brain phosphatidylethanolamine (PE) (Avanti Polar Lipids, Inc., Pelham, AL) with gangliosides G_{D1a} and G_{T1b} (8.8:4.4:1:1 wt/wt) on a 150-μm hole in black Teflon film using a brush technique (Needham and Haydon, 1983). Lipids and gangliosides (Sigma Chemical Co.) were used as received. Squalene (Aldrich Chemical Co., Milwaukee, WI) was passed through an activated aluminum oxide column and stored under argon at 4°C. The bilayer chamber was mounted on a temperature controlled stage of an inverted microscope (Nikon Diaphot, Garden City, NY). The membranes, maintained at 35–37°C, were bathed by symmetrical 140 mM NaCl, 2.5 mM KCl, 5 mM $MgCl_2$, 2 mM $CaCl_2$, 1 mM PIPES, pH = 6.3 solutions.

Optical Measurements

The planar membrane and attached cells were imaged with an 11 mm working distance, MPlan 20X/0.4 NA, ELWD objective (Nikon) and projection lens (2.5 X, Nikon) onto the face of a video camera (SIT 66; Dage-MTI Co., Michigan City, IN), displayed on a monitor, and

recorded on VHS format tape (recorder model SLV-393, Sony Communications Co., Parsippany, NJ). For epi-fluorescence experiments detecting ethidium bromide intercalating DNA, a neutral density filter (ND8 Nikon) and filter cube (G2A Nikon, ex 510–560 nm, dichroic mirror 580 nm, em > 590 nm) were used. The resulting fluorescence intensity changes were measured with a photodiode (EG and G, Salem, MA) applied to the face of the video monitor at the site of the cell of interest (the diameters of the nuclei subtended on the screen exceeded the active area of the photodiode). The fluorescence signal and ΔY_{90} (see Electrical Measurements) were synchronized and digitized for further analysis.

Electrical Measurements

The horizontal planar bilayer was voltage clamped with a locally constructed current amplifier (25 kHz bandwidth with a 150-pF input capacitance, designed by R. Levis, Rush Medical College, Chicago, IL). Ag-AgCl electrodes made contact with the aqueous compartments via agar bridges. A sinewave of frequency, f, 803 Hz or 103 Hz, amplitude 10 mV p-p, superimposed on a constant holding potential (usually 10 mV) was applied as a command voltage to the bottom (*trans*) solution bathing the membrane, with the top (*cis*) solution grounded. The changes in output current were converted into in-phase, ΔY_0, and out-of-phase, ΔY_{90}, components with respect to the applied sinewave by a two phase lock-in amplifier (EG and G model 5208; Princeton, NJ) set to a 3-ms time constant (30 ms for 103 Hz sinewave). ΔY_0 and ΔY_{90} currents were converted (see below) into their natural units of conductance (nS) and capacitance (pF), respectively. The initial capacitance of the planar bilayer as well as subsequent slow drifts were regularly compensated. The direct current admittance (i.e., conductance), Y_{dc}, was measured by lowpass filtering (8-pole Bessel, Model 902, Frequency Devices, Haverhill, MA) the voltage clamp amplifier output at 200 Hz for the 803 Hz sinewave and at 25 Hz for the 103 Hz sinewave. ΔY_0, ΔY_{90}, and ΔY_{dc} signals were recorded with a four-channel FM tape recorder (Racal 4DS, Sarasota, FL). As required, these signals were amplified, filtered, and digitized with 12-bit resolution (Axolab-1, Foster City, CA).

Calibration

Because the series resistance, R_s, was small (10–20 kΩ with agar bridges), stable (measured variation <5 Ω/min), and much less than the cell impedance ($1/\omega C$) the phase-angle did not drift and could be accurately set (e.g., $B^2 = 1$ in Eq. 3 *a* of Joshi and Fernandez, 1988).[1] The phase-angle was adjusted until 20 pF changes introduced with the capacitance compensation circuitry of the voltage clamp amplifier did not produce changes in Y_0 (Neher and Marty, 1982). In a typical experiment, 2–3 cells of the 15–30 adhered cells fused to the planar membrane, causing less than a 50% increase in the initial capacitance of ≈120 pF. Currents were converted to conductances by dividing by the amplitude of the sinusoidal voltage. The out-of-phase conductance was in turn converted to units of capacitance by dividing by the angular frequency, $\omega = 2\pi f$. The overall procedure was calibrated with fixed resistors (Kobra, K and M Electronics, West Springfield, MA) and a decade capacitor unit (type 1412-BC, General Radio, Concord, MA) wherein capacitances could be varied with 1 pF gradations. As the input load capacitance was incremented by 1 to 50 pF, Y_{90} increased linearly. The calibration was

[1] Control experiments using ¾ m thick (≈18 μm) Teflon as a fixed capacitor in the bilayer chamber established that R_s hardly varied over long times. Although R_s was small, it did cause an in-phase, Y'_0, signal because of the small voltage drop across it: $Y'_0 = \omega^2 C^2 R_s/(1 + \omega^2 C^2 R_s^2)$. Because $Y'_0 = R_s\omega^2 C^2$ for $R_s \ll 1/\omega C$, Y'_0 was sensitive to bilayer capacitance drift. Thus, the bilayer capacitance was regularly compensated and monitored throughout the course of an experiment. To calculate the final g_p, we subtracted Y'_0 from the final Y_0 component after cell fusion.

independent of the input load capacitance (range 50–200 pF). ΔY_0 and ΔY_{dc} were in agreement when fixed resistors were used.

The main potential source of error in this system is increases in Y_{dc} unrelated to the fusion pore. We refer to these changes in bilayer conductance, which contaminates ΔY_0, as "nonspecific." Because these increases only occurred under fusogenic conditions, they correlated with membrane fusion. But they were neither required for, nor caused by, fusion. Subtracting ΔY_{dc} from ΔY_0 (Spruce et al., 1989) would eliminate conductance due to the planar membrane and would give a properly corrected ΔY_0 only if the conductance of the fusing cell was negligible. However, the conductances of some cells were significant (Melikyan, Niles, and Cohen, 1993). In this paper we only considered experiments with negligible, if any, Y_{dc} changes. In the companion paper (Melikyan et al., 1993), we quantitatively account for the consequences of cell conductances.

RESULTS

Electrical Features of Cell-Bilayer Fusion

The simplified equivalent circuit describing fusion of a cell to the planar membrane is the cell capacitance, C_c, in series with the fusion pore conductance, g_p (Fig. 1 *A*), as used for secretory granule-plasmalemma fusion (Zimmerberg et al., 1987; Breckenridge and Almers, 1987; Alvarez de Toledo and Fernandez, 1988) and for transfected fibroblast-erythrocyte fusion (Spruce et al., 1989, 1991). The admittance of the planar bilayer is not considered because its conductance was negligible and its capacitance was compensated. ΔY_0 and ΔY_{90} are as originally given in Zimmerberg et al. (1987):

$$\Delta Y_{90} = (g_p^2 \omega C_c)/(g_p^2 + \omega^2 C_c^2) \quad (1)$$

$$\Delta Y_0 = (g_p \omega^2 C_c^2)/(g_p^2 + \omega^2 C_c^2) \quad (2)$$

Qualitatively, immediately upon fusion the pore conductance is small, the voltage drops predominantly across the pore, and the current is not phase shifted. Thus, small pores are recorded by ΔY_0, but not by ΔY_{90} (Fig. 1 *C*). As the pore dilates, the voltage drops increasingly across C_c, and the current is progressively phase shifted toward 90°. Thus, ΔY_{90} rises monotonically with increasing g_p. ΔY_0 initially rises with g_p because the total current increases as the limiting pore conductance increases. When g_p has grown so as not to be the limiting impedance element, the circuit increasingly approximates a capacitor and the in-phase current approaches zero (Fig. 1 *B*).

The large cell admittance, arising from the large C_c, causes several noteworthy consequences for measurements. Firstly, small fusion pores and their flickers are directly measured by $\Delta Y_0 = g_p$ for fusion pores up to 15 nS (for $f \geq 803$ Hz, Fig. 1 *C*). In fact, ΔY_0 yields g_p regardless of the precise value of C_c (Fig. 1 *D*). Secondly, even when g_p is as large as 3 μS, Y_0 does not return to baseline (Fig. 1 *B*), because a measurable fraction of the voltage still drops across g_p. For example, the admittance of the cell ωC_c = 100 nS for C_c = 20 pF and f = 800 Hz. If g_p = 500 nS, 16% of the applied voltage still drops across it and ΔY_0 is not zero. Thus, ΔY_0 gives g_p for large and small pores. Both ΔY_0 and ΔY_{90} determine intermediate values of g_p. Thirdly, when the applied voltage partially drops across the final g_p, the steady state value of

ΔY_{90} underestimates C_c. C_c is correctly calculated by accounting for the voltage-dividing effect. Fourthly, while ΔY_{90} is not sensitive to small pores (Fig. 1 *C*) or changes in g_p above a few hundred nS (Fig. 1 *B*), it is not corrupted by nonspecific Y_{dc} increases and, hence, is more reliable in these cases than ΔY_0.

Basic Phenomenon

About 10 μl of the concentrated cell suspension infected with either PR8 (PR8MDCK) or Japan57 (J57MDCK) viruses was sedimented onto the horizontal planar mem-

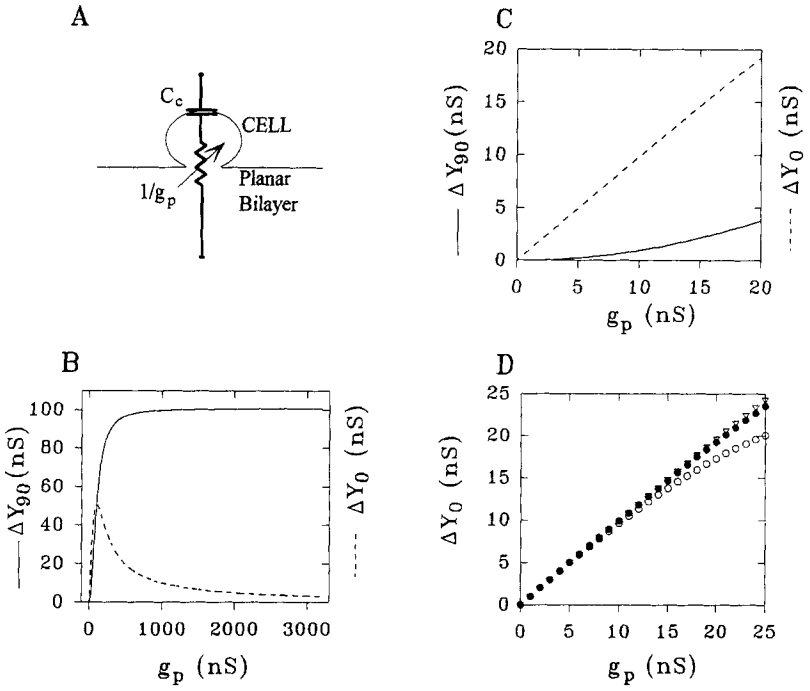

FIGURE 1. ΔY_0 and ΔY_{90} determine g_p. (*A*) Equivalent circuit of cell-bilayer fusion. C_c is cell membrane capacitance, g_p denotes fusion pore conductance. (*B*) ΔY_{90} (*solid curve*) and ΔY_0 (*dashed curve*) as functions of g_p according to Eqs. 1 and 2, for C_c = 20 pF, f = 803 Hz. (*C*) Same as in *B*, but limited to small g_p. Note that small g_p = ΔY_0. (*D*) For small pores, g_p = ΔY_0 independent of the cell capacitance; C_c = 10 pF (*open circles*), 20 pF (*filled circles*) and 30 pF (*triangles*).

brane. 4 min after 15–30 cells established contact with the bilayer, the pH was lowered by injecting 25 μl of concentrated isotonic succinate buffer (pH = 4.9) directly over the planar membrane without stirring. This acidified the solution near the bilayer within 1–3 s as determined by monitoring the membrane conductance with symmetrically placed 50 μM of the protonophore uncoupler carbonylcyanide *p*-trifluoromethoxyphenylhydrazone (FCCP). This change of pH was assured because the higher density succinate buffer rapidly settled on the teflon partition and

replaced the pH 6.3 solution. This settling was directly visualised by adding trace 6-carboxyfluorescein to the pH 4.9 succinate buffer.

After 27 ± 7 s (mean ± SEM, n = 21, PR8MDCK), the first changes in admittance were detected. Typical out-of-phase, ΔY_{90}, and in-phase, ΔY_0, responses as well as ΔY_{dc} are shown in Fig. 2 *A*. The nonzero steady state value of the biphasic ΔY_0,

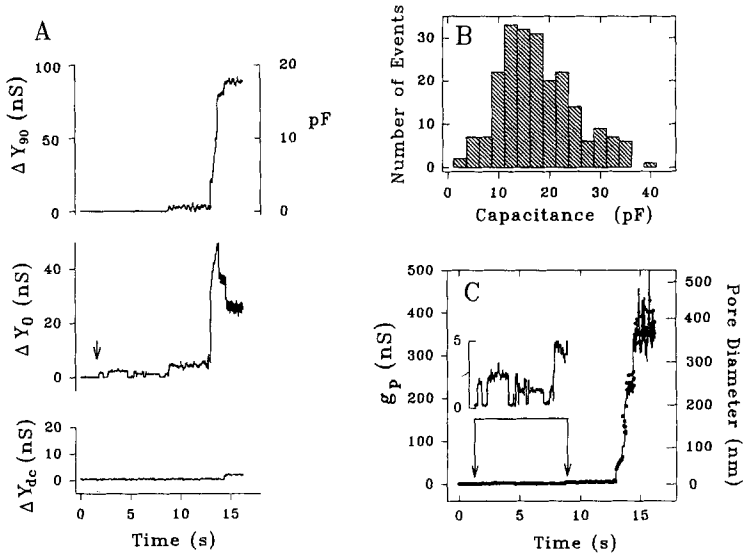

FIGURE 2. The basic electrical response. (*A*) ΔY_{90}, ΔY_0, and ΔY_{dc} traces upon cell-planar bilayer fusion. 26 J57MDCK cells were sedimented on top of a horizontal planar bilayer. A sinewave of frequency f = 803 Hz, amplitude 10 mV *p–p*, superimposed on a 10-mV holding potential was applied. The record shown starts 72 s after the top solution was acidified. The arrow corresponds to the first detected increase in ΔY_0. Note that ΔY_{90} has not changed at this point. (*B*) Fusing cell capacitance histogram obtained from the steady-state values of ΔY_{90} for J57MDCK. This histogram represents all experiments (n = 219), regardless of ΔY_{dc} changes, because the final ΔY_{90} is not corrupted by ΔY_{dc}. The left part of the distribution does not correspond to the cell capacitance and presumably results from incomplete fusion pore opening. The largest values of C_c are probably due to cells fusing amongst themselves as well as to the bilayer, as directly observed in ethidium fluorescence experiments (data not shown). (*C*) g_p calculated from ΔY_{90} (*solid curve*) and ΔY_0 (*circles*) of *A*, where C_c = 18 pF obtained from the final ΔY_{90} after accounting for the small voltage drop across the final fusion pore. The right-hand ordinate converts the fusion pore conductance into its approximate diameter (Hall, 1975) by modeling the pore as a right cylinder with specific resistivity of 100 Ω-cm and length of 15 nm. This model is as previously assumed (Spruce et al., 1989), thereby facilitating comparisons with pore diameters calculated in other systems. The inset displays g_p at a finer conductance scale (nS) for the time interval shown by the double arrows.

yielded a finite final pore conductance which was comparable to the cell capacitative admittance. The fusing cell capacitance histogram determined from the final value of ΔY_{90} was broad (Fig. 2 *B*). The dispersion is due to the MDCK cell size variation, to HA-induced cell-cell fusion (see Fig. 2, *legend*) upon acidification, and possibly to

some fusion events wherein the fusion pore did not enlarge appreciably. The mean value, ~17 pF, is in accord with the size of MDCK cells. The pore conductance g_p determined from ΔY_0 (*filled circles*) and ΔY_{90} (*solid line*) currents, using Eqs. 1 and 2, is shown in Fig. 2 *C*. The equivalency in g_p, independently calculated from the ΔY_0 and ΔY_{90}, supports the validity of the equivalent circuit of Fig. 1 *A*.

Parameters Affecting Fusion

MDCK cell-planar bilayer fusion efficiency varied between infected cell preparations, with, maximally, 10–15% of the adhered cells fusing and their fusion pores fully opening. Fusion was temperature and pH dependent. At pH $\geq$6.3, 37°C or at pH 4.9, 22°C, neither Y_{90} nor Y_0 (nor ΔY_{dc}) changes were observed within 30 min. Fusion of cells to bilayers also required cleaved HA as in other fusion systems (Klenk, Rott, Orlich, and Blodorn, 1975; White et al., 1982). HAb2 cells expressing uncleaved HA0 glycoprotein (Sambrook, Rodgers, White, and Gething, 1985) neither fused nor caused any changes in admittance. After cleaving HA0 with trypsin (Ellens et al., 1990), HAb2 cells were fusion competent at low pH. This control could not be effectively performed with our line of MDCK cells, presumably because endogeneous cell proteases cleaved the HA0 (van Meer and Simons, 1983). Also, noninfected MDCK cells did not fuse: neither admittance nor ethidium bromide fluorescence increases were observed under fusogenic conditions.

Gangliosides, which are receptors for HA due to their terminal sialates (Suzuki et al., 1986), increased the efficiency of fusion and decreased the time to fusion as elaborated in the companion paper (Melikyan et al., 1993). If the infected MDCK cells were allowed to make contact with the planar membrane for longer than the typical 4 min protocol (15 min and over) before acidifying, fusion was inhibited. As the cells are expressing the viral neuraminidase as well as HA, hydrolysis of the gangliosides would account for this time-dependent inhibition. Prolonged exposure to low pH, before fusion, led to inactivation of fusion for PR8MDCK but not J57MDCK. When J57MDCK cells were settled onto planar membranes bathed by *cis* pH 4.9, 37°C solution, rather than settled in pH 6.3 solution which was acidified after a 4-min adhesion, fusion proceeded. However, PR8MDCK cells did not fuse when introduced into the pH 4.9 solution. This is consistent with substantial inactivation of PR8 virus within 1 min at low pH (Sato, Kawasaki, and Ohnishi, 1983; Yewdell et al., 1983; Wunderli-Allenspach and Ott, 1990), whereas J57 virus is not inactivated by prolonged exposure to low pH (Ellens et al., 1990; Puri, Booy, Doms, White, and Blumenthal, 1990). As it took ~1 min for the cells to settle onto the bilayer, the HA of PR8, but not of J57, was inactivating as the cells settled in low pH.

Mixing of Aqueous Contents upon Fusion

The conclusion that increases in Y_0 and Y_{90} were due to fusion was independently confirmed by examining the spread of an aqueous dye, ethidium bromide, into cells. Ethidium bromide was chosen because its quantum yield is large when bound to DNA, but small when free in solution. (Thus, one expects fluorescence to increase when ethidium gains access to the cell nucleus.) The bright-field image of several cells adhered to a planar membrane is shown (Fig. 3 *a*). Ethidium bromide was included in the solution of the cell-free side (*trans*) before the bilayer was formed. The free

ethidium (0.1–1 mM) did not visibly fluoresce (Fig. 3 *b*). Upon each Y_0 and Y_{90} increase characterizing fusion, an individual cell nucleus became highly fluorescent (Fig. 3, *c* and *d*). The lower panel of Fig. 3 illustrates the temporal correlation between the admittance and fluorescence increases. The electrically detected fully opened pore was always accompanied by a fluorescent signal. The ethidium had to

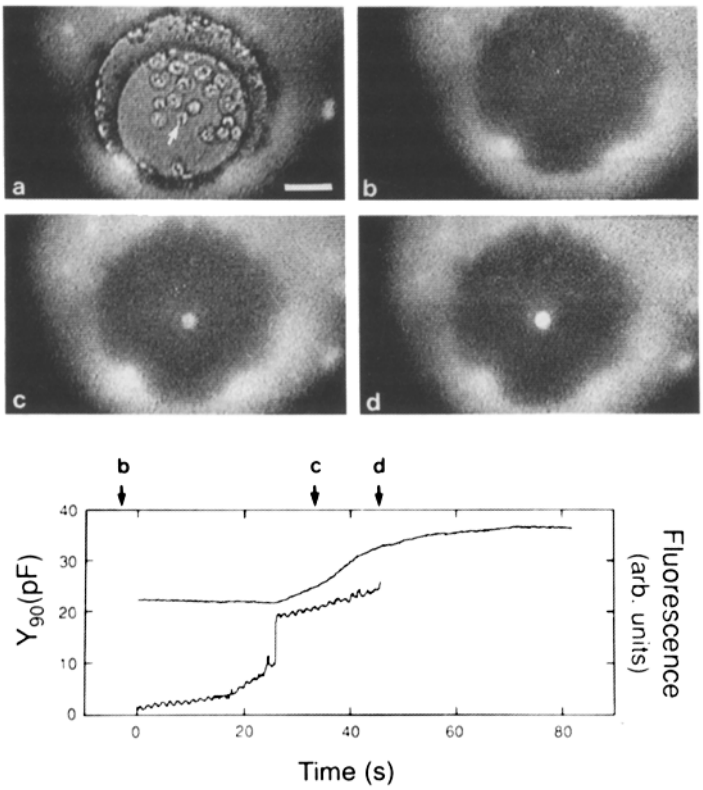

FIGURE 3. Cell-planar membrane fusion monitored by ethidium bromide. (*Top*) (*a*) Bright-field view of J57MDCK cells contacting a horizontal lipid bilayer membrane bathed by a pH 6.3 solution. The arrowhead indicates the cell that will fuse to the lipid membrane. (*b*) Fluorescence micrograph after the pH of the top solution was lowered to 4.9, but before ΔY_{90} increased. (*c*) 6 s after ΔY_{90} increased. (*d*) 19 s after ΔY_{90} increased. The cell-free, bottom pH 6.3 solution contained 1 mM ethidium bromide. Bar, 40 μm. (*Bottom*) The time course of ΔY_{90} (*lower trace*) and fluorescence intensity of the fusing cell (*upper trace*). Arrows marked *b, c,* and *d* correspond to the times of the micrographs.

enter the cell either through the fusion pore from the *trans* solution, or through the cell membrane by ethidium contaminating the *cis* solution (for example, deposited during formation of the planar membrane). To distinguish, we purposely added 0.2 mM ethidium to the *cis* compartment, whereupon 5–10% of the cell nuclei became faintly fluorescent, indicating that some cells were leaky. We then triggered fusion.

The fusing cells, as determined by nuclei becoming highly fluorescent, did not correlate with the leaky cells. Rather, all cells had the same probability of fusing. Thus, the highly fluorescent cells were stained by ethidium entering through the fusion pore.

Flickering

In over 70% of the fusions, the first electrical event was the formation of a small pore that repetitively flickered open and closed. g_p for these early flickering pores was given directly by ΔY_0 (Fig. 4 *A*) and was typically ~1–2 nS. Occasionally pores as

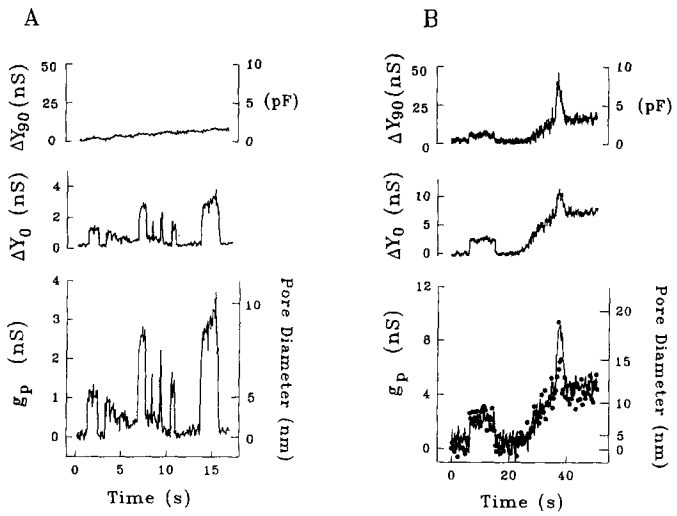

FIGURE 4. Flickering of fusion pores followed by irreversible opening with fluctuating conductances. (*A*) Flickering: an 803 Hz sinewave was superimposed on a 30 mV holding potential. No changes in ΔY_{dc} (not shown) were detected and ΔY_{90} exhibited only slow drift due to planar bilayer sagging. Lower trace shows g_p, calculated from ΔY_0, and approximate equivalent diameter of the pore. (*B*) Detection of pores for a command voltage of 103 Hz sinewave. A larger fraction of the applied voltage drops across C_c for lower frequencies, increasing the sensitivity of ΔY_{90} for small g_p. Lower panel shows g_p calculated from ΔY_0 (*circles*) and ΔY_{90} (*solid line*). g_p continues to fluctuate after the pore irreversibly opens. The capacitance of the fusing PR8MDCK cell was 25 pF. For illustration purposes, only each fifth point of calculated g_p is shown. Right-hand ordinate shows the equivalent diameter of the pore.

small as 270–300 pS (Fig. 5) or as large as tens of nS were recorded (data not shown). The smallest pores are in accord with the initial pore conductances observed both in exocytotic secretion (Breckenridge and Almers, 1987; Spruce et al., 1990) and HA-transfected fibroblast-to-erythrocyte fusion (Spruce et al., 1989, 1991). For the flickering pores of several nS, the conductances could be followed by both ΔY_0 and ΔY_{90}, at sufficiently low (103 Hz in Fig. 4 *B*) stimulating frequencies. The in-phase and out-of-phase currents yielded the same g_p, again supporting the validity of the equivalent circuit (Fig. 1 *A*).

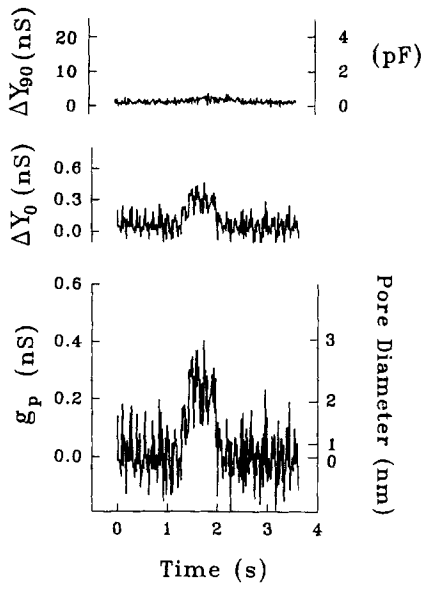

FIGURE 5. Fusion pores with small conductances occasionally occur. This small pore of 270 pS, which eventually fully enlarged, was in accord with the initial conductances seen in mast cell exocytotic secretion and HA-expressing cells to erythrocyte fusion. J57MDCK cells were used in this experiment.

Stages of the Fusion Pore

After the electrically quiescent stage, fusion pores formed and enlarged in three distinct stages: (*a*) repetitive pore flickering, referred to as *R*, lasting on the order of 30 s; (*b*) irreversible dilation to a securely opened pore (*S*) with g_p fluctuations in *S* stage; and (*c*) expansion to a fully opened, terminal *T* stage, relatively stable pore (Fig. 6). Pores left the flickering stage from conductances on the order of 2 nS and entered an irreversibly open, electrically diverse, stage. Within this stage, pore

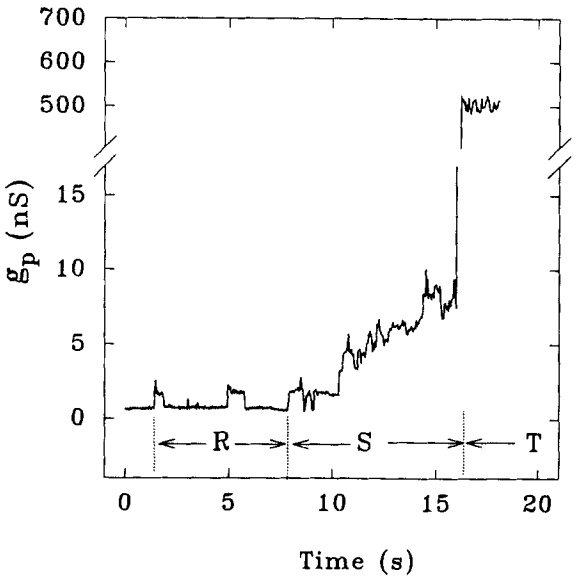

FIGURE 6. Stages of fusion pore dilation. *R* indicates the repetitive flickering stage of fusion. In stage *S*, the pore is securely open and here exhibits fluctuating g_p. The pore leaves stage *S* with a fast expansion to the terminal stage *T*. Fusion pore conductances were calculated only from ΔY_0. J57MDCK with f = 803 Hz, record shown is 58 s after acidification. This experiment was chosen for illustration because its fusion pore passed through stages quickly, aiding visual clarity.

conductances varied widely, from as little as a few nS to as much as 100 nS, and could remain relatively stable, slowly increase, or even fluctuate. This stage of the fusion pore expanded to its fully enlarged state with one to three instantaneous (< 15 ms) step-like rises in g_p, followed by a slower increase (see also Fig. 2 *C*) to a final conductance of 457 ± 166 nS (mean ± SD, n = 17, J57MDCK) corresponding to a diameter of about 475 nm (Hall, 1975). (For g_p > 100 nS, g_p is controlled by the access conductance which varies linearly with diameter.)

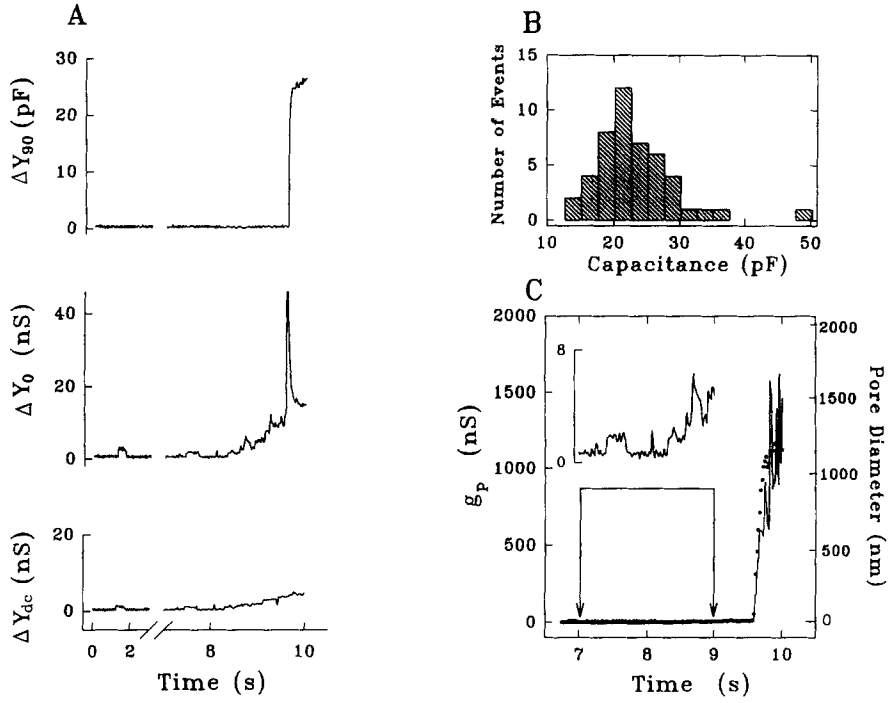

FIGURE 7. Fusion of HAb2 cells to planar membranes. (*A*) Typical ΔY_{90}, ΔY_0 and ΔY_{dc} signals upon fusion with the bilayer membrane (103 s after acidification). Flickering did not occur between the break marks. (*B*) Histogram of C_c for HAb2 cells fusing to planar bilayers (n = 47), obtained as in Fig. 2 *B*. (*C*) Fusion pore conductances and approximate diameters calculated from ΔY_{90} (*solid line*) and ΔY_0 (*circles*). The inset shows the pore flickering within the double arrows on a finer conductance scale.

Fusion Requires Only HA

The infected cells contained preassembled virus particles, about to bud, at the cell surface. Thus, viral proteins other than HA could have contributed to the observed fusion. We therefore repeated the described experiments with HAb2 cells, which stably express ~7 × 10^6 HA trimers per cell (Ellens et al., 1990) but express no other viral proteins. Fig. 7 *A* illustrates ΔY_{90}, ΔY_0, and ΔY_{dc} responses after the *cis*-solution was acidified. Fluorescence experiments with ethidium bromide verified that the

electrical responses were due to fusion (data not shown). The HAb2-bilayer fusion pores exhibited qualitatively similar dynamic features to those of the infected MDCK cells. The quiescent, repetitvely flickering, and securely open stages of the J57MDCK and HAb2 (which express the Japan 57 strain of HA) cells were comparable. However, the final fusion pore conductance (Fig. 7 *C*) was typically several times higher than for infected MDCK cells (Fig. 2 *C*) and the final rapid pore expansion usually occurred in one step (Fig. 7 *C*). The mean final pore conductance for HAb2-bilayer fusion was 1,415 nS ± 188 nS (n = 17); in three experiments g_p was too large to estimate. The cell capacitances determined from the final values of ΔY_{90} agree with those directly measured by patch clamp experiments (Ellens et al., 1990).

DISCUSSION

Advantages and Disadvantages of the Cell-Planar Membrane Model System

This study represents the first rigorous demonstration of fusion of cells to planar bilayer membranes (for previous attempts see Babunashvili and Nenashev, 1982). This model system has advantages that are unique in their combination. Individual events can be studied, the initial and final pore conductances can be directly determined because the cell admittance is large, the lipid composition of the bilayer can be controlled, and receptors can be altered. Fusion of HA expressing cells does not appear to require specific cell types: chicken embryo and human fibrosarcoma cells infected with influenza virus fused to planar membranes in the same manner (data not shown).

The model system complements cell–cell fusion systems wherein the pore is studied by the patch clamp technique (Spruce et al., 1989, 1991). These latter systems have the advantage that the target cell can be varied and with erythrocytes, fusion is 100% efficient. However, forming tight seals are difficult with HA-expressing cells under fusogenic conditions (J. Zimmerberg, personal communication). Also, to obtain reliable pore conductances when two cells with large membrane capacitances fuse, phase settings must be continually updated as the fusion pore expands, which should be possible with the phase tracking technique (Fidler and Fernandez, 1989). The noise-bandwidth product of whole-cell recording is similar to that realized with planar membranes. The root-mean square current noise, I_{rms}, is proportional to $C_m R_s^{0.5}$, where C_m is the cell (or planar membrane) capacitance and R_s is the series resistance (Sigworth, 1983). The bilayer capacitance ($\approx$150 pF) is about ten times larger than cell capacitance ($\approx$15 pF), whereas the bilayer series resistance ($\approx$20 kΩ) is ~100 times smaller than patch pipette resistances ($\approx$2 MΩ).

Currently, the major disadvantage of the cell-bilayer model system is the low efficiency of fusion; it requires that more than one cell be added per bilayer to obtain fusion. We overcame this by adding 20–30 cells per bilayer. However, the extra, nonfusing cells, could contribute to ΔY_{dc}. This would be easily accounted for if ΔY_{dc} were entirely due to conductances within the bilayer, unrelated to fusion: subtracting ΔY_{dc} from ΔY_0 would yield the true in-phase component due to fusion. But the current pathway through the series combination of g_p and cell conductance, G_c, could also be contributing (Melikyan et al., 1993). The same problem of ΔY_{dc} contamination might occur in HAb2-erythrocyte fusion (Spruce et al., 1989, 1991). In that case,

ΔY_{dc} was, in fact, simply subtracted from ΔY_0 with the view that ΔY_{dc} was only due to increases in the HAb2 cell conductance. However, as the red cells were swelling during fusion, the quantitative validity of that approach is not certain. Also, it is well known that HA, under fusogenic conditions, produces permeability increases in the target cell membrane. Fusion of influenza virus to cells is associated with changes in permeabilities of plasma membranes and erythrocyte hemolysis (Patel and Pasternak, 1985; Loyter, Nussbaum, and Citovsky, 1988). Red cell aqueous contents are rapidly released to the extracellular space when fusing to HA-expressing cells (Sarkar, Morris, Eidelman, Zimmerberg, and Blumenthal, 1989). Even isolated aggregates of HA induce permeability changes (Sato et al., 1983). By using multifrequency admittance measurements, g_p and G_c can be determined, relieving the uncertainties. Alternatively, if fusion efficiency were improved, less cells could be added, and nonspecific bilayer conductances would become less frequent.

We assumed that only one pore formed and then expanded for every cell fused to the planar membrane, as was also assumed for data obtained in patch clamp experiments. We reliably calculated the time course of g_p for the first fusion pore. The conductances of subsequent pores were not calculated, because their values would be contaminated by the conductance of a prior pore and/or Y_{dc} changes. While we counted the number of pores that fully expanded, later forming pores could have remained undetected if they did not fully open because the large prior conductances could have obscured their relatively small conductances. In fact, while all cells that became highly fluorescent temporally correlated with a fully opened pore, faintly fluorescent cells could not often be correlated with an electrical signal. These faintly fluorescent cells could have either been leaky or fused, but their pores remained in intermediate stages. Thus, the percentage of cells that fused could be higher than our count.

Pore Dynamics

The times for small fusion pores to fully enlarge in the cell-bilayer system is comparable to fusion pores in HA-expressing cell-erythrocyte (Spruce et al., 1991) and mast cell exocytotic (Curran et al., 1993) systems. However, fusion pores in purely lipid planar bilayer systems enlarge more rapidly: fusion pores between phospholipid vesicles and planar membranes (Cohen et al., 1980) and between two hemispherical bilayers (Melikyan, 1984) expand in < 1 ms. A counterbalancing force in the cells must be opposing the tension of the planar bilayer (Needham and Haydon, 1983) which would otherwise result in quick fusion pore dilations. (In fact, the transition from the *S* to *T* stage is instantaneous.) MDCK cells treated with 40 μg/ml colchicine and 25 μg/ml cytochalasin B for 30 min at 37°C exhibited similar fusion efficiency, initial and final pore conductance, as well as dilation of the pore in stages (Melikyan et al., 1993). This suggests that neither the microtubules nor microfilaments control the evolution of the pore through sequential stages. After treatment, however, there was more and faster flickering before the pore irreversibly opened. The viral M protein, seen as electron-dense layers beneath the plasma membrane of infected cells (Schulze, 1972), also does not appear to retard pore dilation: HAb2 cells which lack *M* protein showed similar pore growth. Pore

expansion might be controlled by the tensions and bending elasticities of the fusing membranes (Nanavati et al., 1992) as well as cellular elements.

Comparison with Other HA-Fusion Systems

The fusion of cells expressing the influenza HA to planar membranes has the characteristics of HA mediated fusion: pH and temperature dependence (e.g., Wiley and Skehel, 1987; Stegmann, White, and Helenius, 1990), and the requirement that the HA0 precursor be cleaved into its disulfide bond-linked HA1 and HA2 subunits (Klenk et al., 1975; White et al., 1982). In addition, gangliosides, which are known receptors for HA, augment fusion.

The fusion pores connecting cells to planar membranes have the qualitative attributes of pores reported for purely biological systems. However, there are quantitative differences. The transient currents associated with charging of erythrocyte membranes, through fusion pores, upon fusion with HAb2 cells indicate that initial pore conductances were ≈ 150 pS. These pores enlarged to ≈ 500 pS within milliseconds where they were observed in time resolved admittance measurements (Spruce et al., 1991). On the same time scale somewhat larger pores of ≈ 1–2 nS are observed in the cell-planar membrane system. Also, the pore of the model system repetitively flickers before securely opening, for all cells tested including HAb2 cells. In contrast, for HAb2 cell-erythrocyte fusion only single, if any, flickering typically occur (Spruce et al., 1989).

The tension of the planar bilayer, on the order of several dyne/cm (Needham and Haydon, 1983), could be responsible for the differences in fusion pore properties. In cells, there is excess membrane area associated with infoldings, suggesting by Laplace's law that the cell membrane is not under tension. The tension of the bilayer could be quickly enlarging initially small pores into the observed 1–2 nS pores and affecting its subsequent growth. It is even possible, that the tension could be the basis for repetitive flickering. Lipid bilayer membrane tubes under tension spontaneously collapse if the radius is less than the length, the precise relation depending on geometry (Melikyan, Kozlov, Chernomordik, and Markin, 1984). If this collapse were occurring for fusion pores, then pores of small radii would quickly close and not be detected. The repetitive flickering would represent pores of comparable radii and lengths. The final pore conductance for J57MDCK was 457 ± 166 nS (mean ± SD, $n = 17$), corresponding to a pore diameter of ~ 475 nm assuming a right cylinder with a length of 15 nm. (It is noteworthy that this final pore size is adequate to allow the full release of the ≈ 100 nm viral nucleocapsid into the infected cell's cytosol.) The cell fused to planar bilayer was, thus, efficiently perfused with the *trans* solution, as documented by the ethidium mixing experiments. Cells did not exhibit morphological changes when viewed in bright-field microscopy. This is in agreement with a small 475-nm diam pore in relation to overall cell size. Similarly, when erythrocytes fused to HAb2 cells, the fusion sites remained discrete and did not enlarge indefinitely as shown by electron and fluorescence microscopic studies (Doxsey et al., 1985). But the cells were effectively perfused through the fusion pore as evidenced by the fact that large proteins as well as dyes loaded into the erythrocytes transferred into the host cytosol (Doxsey et al., 1985; Sarkar et al., 1989; Spruce et al., 1989).

Thus, the conductances of the fusion pore in the model system are consistent with

those of purely biological systems. Further, the progression of fusion pore growth in stages is a true biological phenomenon, not limited to this artificial system. Pore progression by stages has also been found to occur in exocytotic secretion in mast cells (Zimmerberg et al., 1991; Nanavati et al., 1992; Curran et al., 1993). In the companion paper (Melikyan et al., 1993) we quantitatively characterize the growth of pores in stages.

We thank D. Ok for technical assistance, J. White for providing the HAb2 cell stock and the protocol for releasing them from dishes with a trypsin-free medium, and R. Webster for providing the Japan/305/57 virus innoculum. Drs. L.V. Chernomordik, R.S. Eisenberg, R. Levis, E. Rios, and J. Zimmerberg made useful comments on the manuscript.

Supported by NIH grants GM27367 and AI29606.

Original version received 8 February 1993 and accepted version received 20 May 1993.

REFERENCES

Almers, W., and F. W. Tse. 1990. Transmitter release from synapses: does a preassembled fusion pore initiate exocytosis? *Neuron.* 4:813–818.

Alvarez de Toledo, G., and J. M. Fernandez. 1988. The events leading to secretory granule fusion. *In* Cell Physiology of Blood. R. B. Gunn and J. C. Parker, editors. The Rockefeller University Press, New York. 333–344.

Babunashvili, I. N., and V. A. Nenashev. 1982. Erythrocyte membrane incorporation into planar bilayer lipid membranes. *Biofizika.* 27:441–444.

Bentz, J., H. Ellens, and D. Alford. 1990. An architecture for the fusion site of influenza hemagglutinin. *FEBS Letters.* 276:1–5.

Boulan, E. R., and M. Pendergast. 1980. Polarized distribution of viral envelope protein in the plasma membrane of infected epithelial cells. *Cell.* 20:45–54.

Breckenridge, L. J., and W. Almers. 1987. Currents through the fusion pore that forms during exocytosis of a secretory vesicle. *Nature.* 328:814–817.

Brunner, J., C. Zugliani, and R. Mischler. 1991. Fusion activity of influenza virus PR8/34 correlates with a temperature-induced conformational change within the hemagglutinin ectodomain detected by photochemical labeling. *Biochemistry.* 30:2432–2438.

Cohen, F. S., J. Zimmerberg, and A. Finkelstein. 1980. Fusion of phospholipid vesicles with planar bilayer membranes. II. Incorporation of a vesicular membrane marker into the planar membrane. *Journal of General Physiology.* 75:251–270.

Curran, M., F. S. Cohen, D. E. Chandler, P. J. Munson, and J. Zimmerberg. 1993. Exocytotic fusion pores exhibit semi-stable states. *Journal of Membrane Biology.* 133:61–75.

Doms, R. W., A. Helenius, and J. M. White. 1985. Membrane fusion activity of the influenza virus hemagglutinin (The low pH-induced conformational change). *Journal of Biological Chemistry.* 260:2973–2981.

Doxsey, S. J., J. Sambrook, A. Helenius, and J. M. White. 1985. An efficient method for introducing macromolecules into living cells. *Journal of Cell Biology.* 101:19–27.

Ellens, H., J. Bentz, D. Mason, F. Zhang, and J. M. White. 1990. Fusion of influenza hemagglutinin-expressing fibroblasts with glycoprotein-bearing liposomes: role of hemagglutinin surface density. *Biochemistry.* 29:9697–9707.

Fidler, N., and J. M. Fernandez. 1989. Phase tracking: an improved phase detection technique for cell membrane capacitance measurements. *Biophysical Journal.* 56:1153–1162.

Georgiou, G. N., I. E. G. Morrison, and R. J. Cherry. 1989. Digital fluorescence imaging of fusion of influenza virus with erythrocytes. *FEBS Letters.* 250:487–492.

Hall, J. E. 1975. Access resistance of a small circular pore. *Journal of General Physiology.* 66:531–532.

Harter, C., P. James, T. Bachi, G. Semenza, and J. Brunner. 1989. Hydrophobic binding of the ectodomain of influenza hemagglutinin to membranes occurs through the "fusion peptide." *Journal of Biological Chemistry.* 264:6459–6464.

Hoekstra, D., T. de Boer, K. Klappe, and J. Wilschut. 1984. Fluorescence method for measuring the kinetics of fusion between biological membranes. *Biochemistry.* 23:5675–5681.

Huang, R. T. C., E. Dietsch, and R. Rott. 1985. Further studies on the role of neuraminidase and the mechanism of low pH dependence in Influenza virus-induced membrane fusion. *Journal of General Virology.* 66:295–301.

Huang, R. T. C., R. Rott, and H.-D. Klenk. 1981. Influenza viruses cause hemolysis and fusion of cells. *Virology.* 110:243–247.

Joshi, C., and J. M. Fernandez. 1988. Capacitance measurements. An analysis of the phase detector technique used to study exocytosis and endocytosis. *Biophysical Journal.* 53:885–892.

Klenk, H.-D., R. Rott, M. Orlich, and J. Blodorn. 1975. Activation of influenza A viruses by trypsin treatment. *Virology.* 68:426–439.

Lowy, R. J., D. P. Sarkar, Y. Chen, and R. Blumenthal. 1990. Observation of single influenza virus-cell fusion and measurement by fluorescence video microscopy. *Proceedings of the National Academy of Sciences, USA.* 87:1850–1854.

Loyter, A., O. Nussbaum, and V. Citovsky. 1988. Active function of membrane receptors in fusion of enveloped viruses with cell plasma membranes. *In* Molecular Mechanisms of Membrane Fusion. S. Ohki, D. Doyle, T. Flanagan, S. W. Hui, and E. Mayhew, editors. Plenum Publishing Corp., New York. 413–426.

Matlin, K. S., H. Reggio, A. Helenius, and K. Simons. 1981. Infectious entry pathway of influenza virus in a canine kidney cell line. *Journal of Cell Biology.* 91:601–613.

Matlin, K. S., and K. Simons. 1983. Reduced temperature prevents transfer of a membrane glycoprotein to the cell surface but does not prevent terminal glycosylation. *Cell.* 34:233–243.

Melikyan, G. B. 1984. Interaction and Fusion of Lipid Bilayers. PhD thesis, Moscow State University, USSR. 179 pp.

Melikyan, G. B., M. M. Kozlov, L. V. Chernomordik, V. S. Markin. 1984. Fission of bilayer lipid tubes. *Biochimica et Biophysica Acta.* 776:169–175.

Melikyan, G. B., W. D. Niles, and F. S. Cohen. 1993. Influenza virus hemagglutinin-induced cell-planar bilayer fusion: quantitative dissection of fusion pore kinetics into stages. *Journal of General Physiology.* 102:1131–1146.

Monck, J. R., G. Alvarez de Toledo, and J. M. Fernandez. 1990. Tension in secretory granule membranes causes extensive membrane transfer through the exocytotic fusion pore. *Proceedings of the National Academy of Sciences, USA.* 87:7804–7808.

Morris, S. J., D. P. Sarkar, J. M. White, and R. Blumenthal. 1989. Kinetics of pH-dependent fusion between 3T3 fibroblasts expressing influenza hemagglutinin and red blood cells. *Journal of Biological Chemistry.* 264:3972–3978.

Nanavati, C., V. S. Markin, A. F. Oberhauser, and J. M. Fernandez. 1992. The exoctytotic fusion pore modeled as a lipidic pore. *Biophysical Journal.* 63:1118–1132.

Needham, D., and D. A. Haydon. 1983. Tensions and free energies of formation of "solventless" lipid bilayers. *Biophysical Journal.* 41:251–257.

Neher, E., and A. Marty. 1982. Discrete changes of cell membrane capacitance observed under conditions of enhanced secretion in bovine adrenal chromaffin cells. *Proceedings of the National Academy of Sciences, USA.* 79:6712–6716.

Patel, K., and C. A. Pasternak. 1985. Permeability changes elicited by influenza and Sendai viruses: separation of fusion and leakage by pH-jump experiments. *Journal of General Virology.* 66:767–775.

Puri, A., F. P. Booy, R. W. Doms, J. M. White, and R. Blumenthal. 1990. Conformational changes and fusion activity of influenza virus hemagglutinin of the H2 and H3 subtypes: effects of acid pretreatment. *Journal of Virology.* 64:3824–3832.

Sambrook, J., L. Rodgers, J. M. White, and M.-J. Gething. 1985. Lines of BPV-transformed murine cells that constitutively express influenza virus hemagglutinin. *EMBO Journal.* 4:91–103.

Sarkar, D. P., S. J. Morris, O. Eidelman, J. Zimmerberg, and R. Blumenthal. 1989. Initial stages of influenza hemagglutinin-induced cell fusion monitored simultaneously by two fluorescent events: cytoplasmic continuity and lipid mixing. *Journal of Cell Biology.* 109:113–122.

Sato, S. B., K. Kawasaki, and S.-I. Ohnishi. 1983. Hemolytic activity of influenza virus hemagglutinin glycoproteins activated in mildly acidic environments. *Proceedings of the National Academy of Sciences, USA.* 80:3153–3157.

Schulze, I. T. 1972. The structure of influenza virus. II. A model based on the morphology and composition of subviral particles. *Virology.* 47:181–196.

Sigworth, F. J. 1983. Electronic design of the patch clamp. *In Single-Channel Recording.* B. Sakmann and E. Neher, editors. Plenum Publishing Corp., New York. 3–35.

Skehel, J. J., P. M. Bayley, E. B. Brown, S. R. Martin, M. D. Waterfield, and J. M. White. 1982. Change in the conformation of influenza virus hemagglutinin at the pH optimum of virus-mediated membrane fusion. *Proceedings of the National Academy of Sciences, USA.* 79:968–972.

Spruce, A. E., L. J. Breckenridge, A. K. Lee, and W. Almers. 1990. Properties of the fusion pore that forms during exocytosis of a mast cell secretory vesicle. *Neuron.* 4:643–654.

Spruce, A. E., A. Iwata, J. M. White, and W. Almers. 1989. Patch clamp studies of single cell-fusion events mediated by a viral fusion protein. *Nature.* 342:555–558.

Spruce, A. E., A. Iwata, and W. Almers. 1991. The first milliseconds of the pore formed by a fusogenic viral envelope protein during membrane fusion. *Proceedings of the National Academy of Sciences, USA.* 88:3623–3627.

Stegmann, T., J. M. Delfino, F. M. Richards, and A. Helenius. 1991. The HA2 subunit of influenza hemagglutinin inserts into the target membrane prioir to fusion. *Journal of Biological Chemistry.* 266:18404–18410.

Stegmann, T., H. W. M. Morselt, J. Scholma, and J. Wilschut. 1987. Fusion of influenza virus in an intracellular acidic compartment measured by fluorescence dequenching. *Biochimica et Biophysica Acta.* 904:165–170.

Stegmann, T., S. Nir, and J. Wilschut. 1989. Membrane fusion activity of influenza virus. Effects of gangliosides and negatively charged phospholipids in target liposomes. *Biochemistry.* 28:1698–1704.

Stegmann, T., J. M. White, and A. Helenius. 1990. Intermediates in influenza induced membrane fusion. *EMBO Journal.* 9:4231–4241.

Suzuki, Y., Y. Nagao, H. Kato, M. Matsumoto, K. Nerome, K. Nakajima, and E. Nobusawa. 1986. Human influenza A virus hemagglutinin distinguishes sialyloligosaccharides in membrane-associated gangliosides as its receptor which mediates the adsorption and fusion process of virus infection. *Journal of Biological Chemistry.* 261:17057–17061.

Van Meer, G., and K. Simons. 1983. An efficient method for introducing defined lipids into the plasma membrane of mammalian cells. *Journal of Cell Biology.* 97:1365–1374.

Weis, W., J. H. Brown, S. Cusack, J. C. Paulson, J. J. Skehel, and D. C. Wiley. 1988. Structure of the influenza virus haemagglutinin complexed with its receptor, sialic acid. *Nature.* 333:426–431.

White, J. M. 1992. Membrane fusion. *Science.* 258:917–924.

White, J. M., A. Helenius, and M.-J. Gething. 1982. Haemagglutinin of influenza virus expressed from a cloned gene promotes membrane fusion. *Nature.* 300:658–659.

White, J. M., M. Kielian, and A. Helenius. 1983. Membrane fusion proteins of enveloped viruses. *Quarterly Review of Biophysics.* 16:151–195.

White, J. M., and I. A. Wilson. 1987. Anti-peptide antibodies detect steps in a protein conformational change: low-pH activation of the influenza virus hemagglutinin. *Journal of Cell Biology.* 105:2887–2896.

Wiley, D. C., and J. I. Skehel. 1987. The structure and function of the hemagglutinin membrane glycoprotein of influenza virus. *Annual Review of Biochemistry.* 56:365–394.

Wilson, I. A., J. J. Skehel, and D. C. Wiley. 1981. Structure of the haemagglutinin membrane glycoprotein of influenza virus at 3 Å resolution. *Nature.* 289:366–373.

Wunderli-Allenspach, H., and S. Ott. 1990. Kinetics of fusion and lipid transfer between virus receptor containing liposomes and influenza viruses as measured with the octadecylrhodamine B chloride assay. *Biochemistry.* 29:1990–1997.

Yewdell, J. W., W. Gerhard, and T. Bachi. 1983. Monoclonal anti-hemagglutinin antibodies detect irreversible antigenic alterations that coincide with the acid activation of influenza virus A/PR/834-mediated hemolysis. *Journal of Virology.* 48:239–248.

Yoshimura, A., K. Kuroda, K. Kawasaki, S. Yamashina, T. Maeda, and S.-I. Ohnishi. 1982. Infectious cell entry mechanism of influenza virus. *Journal of Virology.* 43:284–293.

Yoshimura, A., and S.-I. Ohnishi. 1984. Uncoating of influenza virus in endosomes. *Journal of Virology.* 51:497–504.

Zimmerberg, J., M. Curran, and F. S. Cohen. 1991. A lipid/protein complex hypothesis for exocytotic fusion pore formation. *Annals of the New York Academy of Science.* 635:307–317.

Zimmerberg, J., M. Curran, F. S. Cohen, and M. Brodwick. 1987. Simultaneous electrical and optical measurements show that membrane fusion precedes secretory granule swelling during exocytosis of beige mouse mast cells. *Proceedings of the National Academy of Sciences, USA.* 84:1585–1589.